Phys. Status Solidi B **251**, No. 8, 1590–1595 (2014) / **DOI** 10.1002/pssb.201451092

physica status solidi b
www.pss-b.com
basic solid state physics

Ultrasonic exploration of vacancy centres with the Jahn–Teller effect: Application to the ZnSe crystal

N. S. Averkiev[1], I. B. Bersuker[2], V. V. Gudkov[3,4], K. A. Baryshnikov[*,1], G. V. Colibaba[5], I. V. Zhevstovskikh[3,6], V. Yu. Mayakin[3], A. M. Monakhov[1], D. D. Nedeoglo[5], M. N. Sarychev[3], and V. T. Surikov[7]

[1] Ioffe Physical-Technical Institute, Russian Academy of Sciences, 26 Polytekhnicheskaya St., St.-Petersburg 194021, Russia
[2] Institute for Theoretical Chemistry, The University of Texas at Austin, 105 E. 24-th St., Stop A5300, Austin, TX 78712-1224, USA
[3] Ural Federal University named after the first President of Russia B.N. Yeltsin, 19 Mira St., Ekaterinburg 620002, Russia
[4] Russian Vocational Pedagogical University, 11 Mashinostroiteley St., Ekaterinburg 620012, Russia
[5] Moldova State University, 60 A. Mateevici St., Chisinau MD-2009, Moldova
[6] Institute for Metal Physics, Ural Division of the Russian Academy of Sciences, 18 S. Kovalevskaya St., Ekaterinburg 620990, Russia
[7] Institute of Solid State Chemistry, Ural Division of the Russian Academy of Sciences, 91 Pervomaiskaya St., Ekaterinburg 620990, Russia

Received 5 March 2014, revised 20 May 2014, accepted 28 May 2014
Published online 3 July 2014

Keywords elastic moduli, Jahn–Teller effect, relaxation, ultrasound, vacancies, ZnSe

* Corresponding author: e-mail barysh.1989@gmail.com, Phone: +7 812 2927155, Fax: +7 812 2971017

We show that the structure, properties, and concentration of vacancies in crystals can be studied by ultrasonic experiments previously employed for impurity centres only. Measurements of the temperature dependence of attenuation and phase velocities of ultrasonic shear waves of 52 MHz propagating along the crystallographic axis [110] of nominally pure ZnSe single crystals (grown by the seeded physical vapour transport method) show strong anomalies which are typical for relaxation processes in system with isolated Jahn–Teller (JT) centres. The observed JT distortion mode is trigonal, subject to a threefold orbitally degenerate T-term interaction with trigonal and tetragonal nuclear displacements. In the absence of sufficiently high concentrations of impurity atoms with such properties we attributed the observed JT centres to zinc vacancies. The temperature dependence of the isothermal and adiabatic forms of the appropriate elastic modulus and the relaxation time show that the relaxation mechanism changes from thermal activation at higher temperatures to tunnelling through a potential energy barrier below 18 K. We provide an estimate of the magnitude of the potential barrier, as well as the pseudorotation frequency and concentration of vacancies. Also we determine the extremum points of the adiabatic potential energy surface of the vacancy centre.

1 Introduction Recent investigations of the III–V:3d and II–VI:3d crystals demonstrated the efficiency of ultrasonic experiments in obtaining new information about the structure and properties of impurity centres, especially the parameters of the Jahn–Teller (JT) effect (JTE) [1] (see [2], and references therein). Ultrasonic measurements reveal the active JT distortion modes, as well as several other characteristics of the adiabatic potential energy surface (APES) of the impurity centre, including linear vibronic coupling constants, the symmetry of the distorted configurations and the energy barrier between them, as well as the frequency of internal pseudorotations that determine high-temperature relaxations. This in turn allows one to reveal the mechanisms of relaxation and the temperature dependence of the relaxation time. Not only impurity atoms but also vacancies in the regular lattice may be subject to the JTE. Such JT centres were detected in Si [3, 4], ZnSe [5–7], and GaAs [8] by means of optical spectroscopy measurements showing that the JT centres in these systems are trigonal distorted. The theory of JT vacancies was developed for II–VI and III–V compounds in [9]. In crystals with sphalerite crystallographic structure the JT centre consists of the vacancy and its nearest neighbours in a tetrahedral coordination with a threefold degenerate T state interaction with t_2 vibrational

modes [9] which produces the $T \otimes t_2$ or $T \otimes (e + t_2)$ JT problems [1]. The electronic wave functions were taken as linear combinations of corresponding atomic functions and, using a phenomenological Hamiltonian, the APES was evaluated for specific values of the linear vibronic constants and crystal fields. In Ref. [10] oxygen impurity atoms were considered as a possible cause of formation of Zn vacancies, and the electronic structure of oxygen-doped ZnSe crystal was studied in Ref. [11].

In the present paper, we report the results of experimental study of the ZnSe crystal using ultrasonic techniques. We found strong anomalies in the temperature dependences of ultrasound attenuation and phase velocity which we interpreted as relaxations in JT centres produced by independent V_{Zn}^{-} vacancies. The relaxation time and relaxed, unrelaxed, and dynamic moduli were constructed as functions of temperature. We proved that the global minima of the APES have trigonal symmetry; the full JTE problem for V_{Zn}^{-} centres in ZnSe is thus $T \otimes (e + t_2)$ including the vibronic interaction of the threefold degenerate T term with both trigonal and tetragonal modes [1]. We obtained the magnitudes of the potential barrier between the minima of the APES, $V_0 = 26.1 \pm 0.7$ meV and the relaxational (vibronic pseudorotational) frequency, $\nu_0 = (0.88 \pm 0.18) \times 10^{12}$ Hz. In combination with the numerical values of the JT stabilization energy ($E_{JT}^{T} = -350$ meV) [5] and the linear vibronic coupling constant ($F_T = -1.6$ eV/Å) [7] derived from optical experiments we estimated also the positions of the orthorhombic and tetragonal saddle points on the APES, as well as the concentration of vacancies ($n = 0.5 \times 10^{17}$ cm^{-3}).

2 Experiment Specimens used in our study were prepared in Moldova State University by the seeded physical vapour-transport method in vacuum [12]. Experiments were carried out on a set-up operating as a variable frequency bridge [13]. The ultrasonic waves were generated and registered by $LiNbO_3$ piezoelectric transducers with the fundamental resonant frequency of $\omega/2\pi \approx 52$ MHz. They propagated along the ⟨110⟩ axis. The latter was chosen because in this direction the two shear normal modes, the slow (polarised along the $\langle 1\bar{1}0 \rangle$ axis) and the fast (⟨001⟩) ones, generate distortions of different symmetry, tetragonal and trigonal respectively. Consequently, the elastic moduli, tetragonal $c_s = (c_{11} - c_{12})/2$ and trigonal $c_f = c_{44}$, can be measured as functions of temperature. The local vibronic mode of tetragonal E-type manifests itself in the attenuation and velocity of the slow shear and longitudinal modes, whereas the local mode of the trigonal T-type is shown in the anomalies of the fast and longitudinal modes.

3 Results The results of the measurements are shown in Figs. 1 and 2. There is a maximum of attenuation for the fast shear mode at $T_m = 34$ K (Fig. 1) and the step-like variation of c_{44} (curve 2 in Fig. 2) superimposed on monotonic back-ground dependences. Such anomalies are typical for relaxation process. The fact that the relaxation anomalies

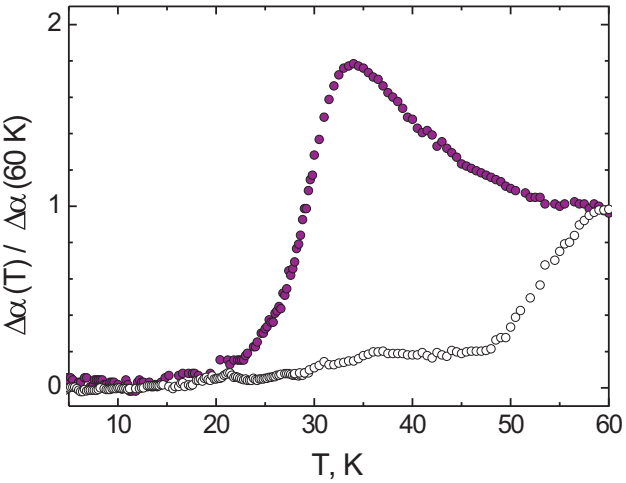

Figure 1 Temperature dependence of attenuation of the ultrasonic waves propagating in ZnSe along the ⟨110⟩ crystallographic axis at 52 MHz. Filled and unfilled symbols relate to the fast and slow modes, respectively.

are observed in the fast shear mode confirms the trigonal type of the JT distortions found earlier in photoluminescence experiments [5, 6].

To extract the relaxation attenuation $\alpha_r = \alpha - \alpha_b$ from the total one, the background attenuation was approximated by the function $\alpha_b(T) = (0.0138 \times T)^2 + (0.0126 \times T)^4$ (see Fig. 3). The data on $\alpha_r(T)$ enable us to reveal the temperature dependences of the relaxation time τ as well as relaxed c^R and unrelaxed c^U moduli. Initially, such a procedure was developed for investigation of the JTE in ZnSe:Ni^{2+} [14], and later it was described in more detail in [2]. It is based on the

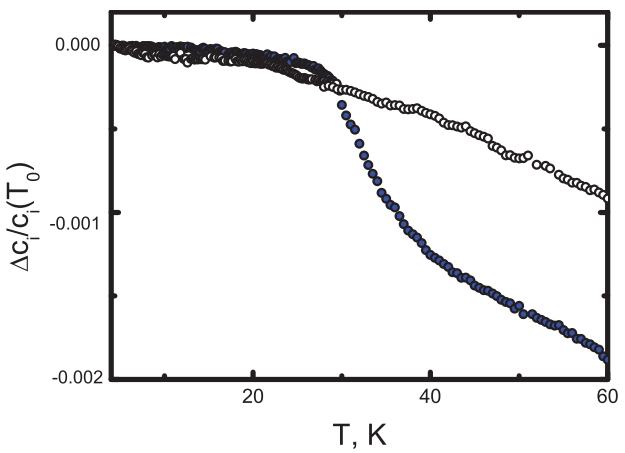

Figure 2 Temperature dependences of elastic moduli in ZnSe measured at 52 MHz. $\Delta c_i = c_i(T) - c_i(T_0)$, $T_0 = 4.2$ K. Filled and unfilled symbols denote $c_i = c_f = c_{44}$ and $c_i = c_s = (c_{11} - c_{12})/2$ values, respectively.

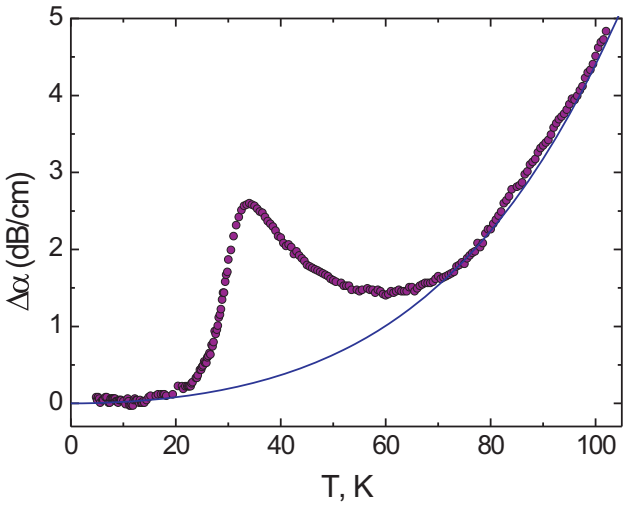

Figure 3 Temperature dependence of attenuation of the fast ultrasonic mode (filled symbols) and the background attenuation fitting curve given by the function $\alpha_b(T) = (0.0138 \times T)^2 + (0.0126 \times T)^4$.

formulas:

$$\tau = \frac{1}{\omega}\left[\frac{\alpha_r(T_1)T_1}{\alpha_r(T)T} \pm \sqrt{\left(\frac{\alpha_r(T_1)T_1}{\alpha_r(T)T}\right)^2 - 1}\right], \quad (1)$$

$$\frac{c_i^U - c_0}{c_0} = \frac{\Delta c_i}{c_0} + 2\frac{\alpha_r}{k_0}\frac{1}{\omega\tau}, \quad (2)$$

$$\frac{c_i^R - c_0}{c_0} = \frac{\Delta c_i}{c_0} - 2\frac{\alpha_r}{k_0}\omega\tau, \quad (3)$$

where index i can refer to the fast ($i = \mathrm{f}$) or to the slow ($i = \mathrm{s}$) mode respectively, T_1 is the temperature corresponding to the condition $\omega\tau = 1$ which is determined as the point of the maximum of the function $f(T) = \alpha_r(T) \cdot T$ on the T-scale. In our case $c_i = c_\mathrm{f} = c_{44}$ is the dynamic (frequency dependent) elastic modulus, $c_\mathrm{f}^U = c_{44}^U$, $c_\mathrm{f}^R = c_{44}^R$, $c_0 = c_{44}(T_0)$, $k_0 = \omega/v_0$, v is phase velocity, $v_0 = v(T_0)$, and $T_0 = 4.2$ K is the reference temperature. The results of applying the Eqs. (1)–(3) to the experimental data are shown in Figs. 4 and 5.

4 Discussion Figure 5 clearly shows the transformation of the dynamic modulus (filled circles) from the relaxed (filled triangles) to the unrelaxed one (unfilled triangles) by cooling. This transformation occurs in the temperature interval where the peak of attenuation is observed for the fast shear mode. Attenuation of the slow shear mode and the modulus $c_\mathrm{s} = (c_{11} - c_{12})/2$ exhibit monotonic temperature dependences (see Figs. 1 and 2). Together these facts justify the assumption that the relaxation is due to JT centres with trigonal symmetry of the global minima of the APES. As mentioned above, this means that the JT problem is $T \otimes (e + t_2)$ or its simpler version $T \otimes t_2$ [1]. In the T problem (see Chapter 3.3 in [1]) there are five JT-active

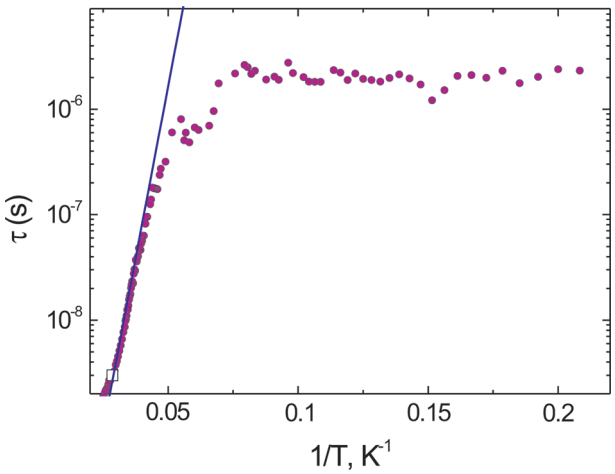

Figure 4 Temperature dependence of relaxation time. The white square corresponds to the condition $\omega\tau = 1$. The line shows the function $\tau(T) = (3\nu_0)^{-1}\exp(V_0/k_\mathrm{B}T)$ with $V_0 = 26.1$ meV and $\nu_0 = 0.88 \times 10^{12}$ Hz.

non-totally symmetric coordinates: two tetragonal (E type: distortions of the tetrahedron along the ⟨100⟩ axes) Q_ε and Q_θ, and three trigonal (T_2 type: distortions of the tetrahedron along the ⟨111⟩ axes) Q_ξ, Q_η and Q_ζ. Three wave functions $|\xi\rangle$, $|\eta\rangle$ and $|\zeta\rangle$ transform as the coordinates products yz, xz and xy, respectively. In linear approximation the vibronic Hamiltonian contains only two vibronic coupling constants F_E and F_T:

$$\hat{W} = \left\| \begin{array}{ccc} F_E\left(\frac{1}{2}Q_\theta - \frac{\sqrt{3}}{2}Q_\varepsilon\right) & -F_T Q_\zeta & -F_T Q_\eta \\ -F_T Q_\zeta & F_E\left(\frac{1}{2}Q_\theta + \frac{\sqrt{3}}{2}Q_\varepsilon\right) & -F_T Q_\xi \\ -F_T Q_\eta & -F_T Q_\xi & -F_E Q_\theta \end{array} \right\|. \quad (4)$$

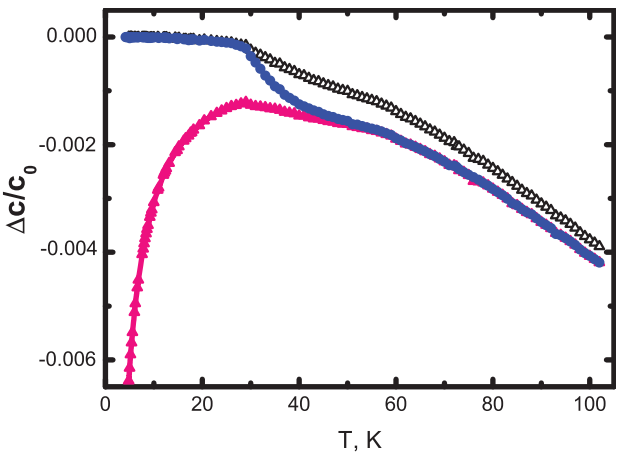

Figure 5 Temperature dependences of the elastic moduli in ZnSe measured at 52 MHz. (c_{44}^U – unfilled triangles, c_{44} – filled circles, c_{44}^R – filled triangles.)

The roots $E_k^v(Q)$ $(k = 1, 2, 3)$ of the secular equations written in the form:

$$\left|\left|\hat{W}_{\gamma\gamma'} - E^v\right|\right| = 0, \quad \gamma, \gamma' = 1, 2, 3, \tag{5}$$

are the three electronic branches of the surfaces in the five-dimensional space Q. In combination with the elastic (non-vibronic) term they determine the three sheets of the APES:

$$E_k(Q) = \frac{1}{2}K_E(Q_\varepsilon^2 + Q_\theta^2) + \frac{1}{2}K_T(Q_\xi^2 + Q_\eta^2 + Q_\zeta^2) + E_k^v(Q), \tag{6}$$

where K_E and K_T are initial (i.e., defined without account of the JTE) force constants. In complete $T \otimes (e + t_2)$ JT problem the APES has 13 extremum points: three tetragonal minima or saddle points ($E = E_{\mathrm{JT}}^E$), four trigonal minima or saddle points ($E = E_{\mathrm{JT}}^T$) and six orthorhombic saddle points ($E = E_{\mathrm{JT}}^O$). Our experiments show that the global minima have trigonal symmetry. In this case tetragonal extremum points are saddle points [1].

Trigonal global minima of the APES were found also in ultrasonic experiments for ZnSe doped by nickel [14] and vanadium [15]. Concentrations of the impurities in the studied crystals were 5.5×10^{19} cm^{-3} and 5.6×10^{18} cm^{-3}, respectively. The peak of attenuation was observed at $T_m \approx 14$ K for nickel impurities at 52 MHz, and it should be below 1.4 K in the case of vanadium at the same frequency (at 156 MHz $T_m \approx 2$ K). To exclude the effect of such transition metal impurities we performed chemical analysis of our specimens. The determination of Cr, Fe, Ni and Cu concentrations in ZnSe crystals was performed using an ELAN 9000 ICP-MS quadrupole-based instrument (Perkin-Elmer SCIEX) with standard operating and acquisition parameters. Samples were dissolved using minimal amounts of HNO3 and then diluted with high pure water up to 100 mg/L for minimizing matrix effects. Solutions of calibrating standards, samples and blanks were introduced pneumatically into ICP by Gem Tip cross-flow nebuliser equipped with Scott-type spray chamber. Isotopes ^{52}Cr, ^{57}Fe, ^{60}Ni and ^{63}Cu were used for monitoring of analytical signals. Relative standard deviation of measured concentrations was about 1−4 %. The results show that the largest concentration of impurities is that of iron, $n_{\mathrm{Fe}} = 5.82 \times 10^{17}$ cm^{-3}. The other detected transition metal impurities that could lead to the JTE have much smaller concentrations. These concentrations of impurities are insufficient for the observation of the ultrasound anomalies [2]. The ZnSe:Fe crystal was investigated earlier [16]; it required much more higher concentrations, namely, $n_{\mathrm{Fe}} = 2.2 \times 10^{19}$ cm^{-3}. Moreover, the JTE in ZnSe:Fe manifests itself in attenuation and phase velocity of the slow shear mode $c_s = (c_{11} - c_{12})/2$ but not in the fast one $c_f = c_{44}$, which we observed in the reported here experiments.

Point defects have been studied by optical detection of magnetic resonance in photoluminescence of ZnSe after electron irradiation of the crystal [6]. A number of defects have been detected in this experiment including zinc vacancies V_{Zn}^-, zinc interstitials, and 25 zinc-interstitial–zinc-vacancy Frenkel pairs with different lattice separations. Except zinc vacancies V_{Zn}^-, all of them have rather low symmetry and no T type terms to be the subject of the JTE $T \otimes (e + t_2)$ problem with trigonal minima observed in our experiments. In combination with the concentrations requirements, outlined above, this led us to the conclusion that the observed anomalies of ultrasound absorption in ZnSe are due to the JT centres created by the V_{Zn}^- vacancies of zinc atoms.

Figure 3 shows the temperature dependence of the relaxation time in the system under consideration obtained using Eq. (1). Such a form of the curve $\tau = \tau(1/T)$ was observed in all ultrasonic experiments on impurity crystals in which the JT centres were 3d elements with degenerate electronic states (see [2] and references therein). Starting from the first investigation [17] of Ni^{3+} in corundum and Mn^{3+} in yttrium aluminum garnet, subject to the $E \otimes e$ problem, the high temperature part is interpreted as due to thermal activation over the adiabatic potential energy barrier V_0, whereas the low temperature part relates to much more slow relaxation caused by quantum tunnelling through the barrier. The approximate expression for the relaxation rate caused by the thermal activation mechanism for the $E \otimes e$ problem is given in [18]:

$$\tau_T^{-1} = 2\nu_0 \exp(-V_0/k_{\mathrm{B}}T), \tag{7}$$

where ν_0 is the is the vibronic 'rotational' frequency (the frequency of pseudorotations of the local distortions along the bottom of the 'Mexican Hat' of the APES [1]). This function can be simulated from the line in the high temperature part. Similarity of the curve given in Fig. 3 to the ones observed for the centres in crystals subject to the $E \otimes e$ problem indicates that in our case we have a similar (in this sense) APES with mountable barriers between the minima. Such a situation can exist in the $T \otimes (e + t_2)$ JT problem in the case of trigonal global minima separated by either orthorhombic or tetragonal saddle points. Anyway, keeping in mind that the number of trigonal minima is four, we can assume a similar to Eq. (7) expression for the thermal activation rate as follows:

$$\tau_T^{-1} = 3\nu_0 \exp(-V_0/k_{\mathrm{B}}T). \tag{8}$$

To estimate the values of V_0 and ν_0 we employed the procedure of fitting Eq. (8) to the experimental curve $\tau = \tau(1/T)$ in the interval of T in which the curve is represented with a line in the semi-logarithmic scale ($1/T = 0.03$–0.038 K^{-1} that corresponds to $T = 26.6$–33 K). The main source of error in evaluation of the function $\tau = \tau(1/T)$ is in the simulation of the temperature dependence of the background attenuation $\alpha_b(T)$. We evaluated this error as a half of the difference between the values obtained under the assumption that $\alpha_b(T)$ is a temperature-independent constant, equal to the attenuation at low temperature of our experiment, $\alpha_b(T) = (0.0138 \times T)^2 + (0.0126 \times T)^4$ (Fig. 4). As a result we get $V_0 = 26.1 \pm 0.7$ meV and $\nu_0 = (0.88 \pm 0.18) \times 10^{12}$ Hz.

The combination of these data with other ones obtained from different experiments or by calculations allows us further to elucidate the structural properties of the vacancies. In particular, the knowledge of the linear vibronic coupling constant makes it possible to determine concentration of the JT centres n. To do it consider the expression for relaxation written in terms of the wave number k_0, frequency dispersion parameter $\omega\tau$, and elastic moduli (see, e.g., expression (7.8) in [2]):

$$\alpha_r = -\frac{1}{2}k_0\frac{(\Delta c_{44}^R)_{\rm JT}}{c_0}\frac{\omega\tau}{1+(\omega\tau)^2}. \tag{9}$$

Here $(\Delta c_{44}^R)_{\rm JT}$ is the contribution of the JT centres to the total relaxed modulus c_{44}. It can be expressed as $(\Delta c_{44}^R)_{\rm JT} = -na_0^2F_T^2/k_{\rm B}T$, where $k_{\rm B}$ is the Boltzmann constant, and a_0 is the Zn–Se interatomic distance. Hence, the expression for ultrasonic attenuation determined at $\omega\tau = 1$ is:

$$\alpha_r(T_1) = \frac{1}{4}k_0\frac{na_0^2F_T^2}{c_0k_{\rm B}T_1}. \tag{10}$$

This equation can be easily solved with respect to the concentration of the vacancy.

$$n = \frac{4c_0k_{\rm B}T_1\alpha_r(T_1)}{k_0a_0^2F_T^2}. \tag{11}$$

Using the magnitudes of $\alpha_r(T_1)\cdot T_1 = 9.25$ Np·K/cm (derived in our experiment), $F_T = -1.6$ eV/Å [7] and $a_0 = 2.46$ Å we obtained $n = 0.5\times10^{17}$ cm^{-3}. The small value of concentration do not provide a contradiction with the stated above proof of a non-impurity character of ultrasound attenuation. Ultrasound attenuation can be observed for such a small concentration of vacancies because the Jahn–Teller effect is very strong in this case. The magnitudes of the energy of the Jahn–Teller stabilization and the constant of the linear vibronic coupling are approximately ten times larger for vacancies than for impurities of the 3d-metal group. Besides, the concentration of vacations in the boron-doped silicon investigated by ultrasonic experiments has been even lower: $\approx 10^{15}$ cm^{-3} [19], 1.5×10^{13} cm^{-3} [20], and 3.1×10^{12} cm^{-3} [21], albeit at essentially higher frequency and lower temperatures.

Note that the $T\otimes(e+t_2)$ problem was considered earlier [22] discussing the result of ultrasonic investigation of the ZnSe:Cr^{2+} crystal. In contrast with the results presented here, the anomalies of attenuation and phase velocity in ZnSe:Cr^{2+} were observed for the slow shear mode. Consequently, the global minima of the APES there are of tetragonal symmetry separated by orthorhombic saddle points. In the case of the JT effect in vacancy centres in ZnSe under consideration in this paper the global minima are of trigonal symmetry separated by tetragonal and orthorhombic saddle points.

The magnitude of the JT stabilization energy is: $E_{\rm JT}^T = -350$ meV [5] (measured from the undistorted tetrahedral configuration). Taking into account the zero point energy in the minima $E_n = \hbar\omega_T(n+3/2)$ and the lowest barrier height between them $V_0 = 26.1$ meV, we can evaluate the position of the lower saddle point: $E_{\rm s} = E_{\rm JT}^T + E_0 + V_0$. Taking $\hbar\omega_T = 11.6$ meV [7], we get $E_{\rm s} = -307$ meV. On the other hand, there is a well-known relation between the energies at the extremum points in $T\otimes(e+t_2)$ problem [1]:

$$E_{\rm JT}^O = \frac{1}{4}E_{\rm JT}^E + \frac{3}{4}E_{\rm JT}^T, \tag{12}$$

meaning that the orthorhombic extremum points make it possible to determine all the extremum points. Together with the data above and the fact that $E_{\rm s}$ describes the lower barrier between the minima we come to the conclusion that the relaxation and tunnelling take place via the orthorhombic saddle points at $E_{\rm s} = E_{\rm JT}^O = -307$ meV with the tetragonal saddle points higher at $E_{\rm JT}^E = -176$ meV. This is one of the rare situations when the experimental data allow one to reveal quantitatively the full picture of the APES of a system with a JT effect $T\otimes(e+t_2)$ problem with numerical estimates of its extremum points and barriers.

5 Conclusion To the best of our knowledge, this paper is the first report of observation and exploration of the JTE in crystal vacancy centres by means of ultrasonic experiments, previously employed for impurity centres only, and the first experimental study of structural and dynamic properties of $V_{\rm Zn}^-$ vacancies in ZnSe crystals, its JTE parameters. By measuring the temperature dependence of ultrasound attenuation and velocity in the fast and slow shear modes propagating along the ⟨110⟩ axis in the pure ZnSe crystal and by analyzing the observed strong anomalies, we reached a full description of the complicated adiabatic potential energy surface of these vacancies with the JT $T\otimes(e+t_2)$ problem, including numerical estimates of the minima and saddle point positions and energy barriers between them, as well as the vibronic (over-the-barrier) pseudorotation frequency and vacancy concentration.

By showing the efficiency of ultrasound measurements in revealing the structure and properties of vacancies in crystals in addition to the previous results obtained for impurity centres, this paper demonstrates also the importance of ultrasound investigations used as a general tool to determine defect properties in crystals. It may also allow one to 'observe the defect in real time', since the typical relaxation time is comparable with the period of the ultrasonic wave.

Acknowledgements The authors appreciate financial support from Russian Foundation for Basic Research (grant No. 12-02-00476-a) and RF President Grant NSh-1085.2014.2. K. A. Baryshnikov is grateful for the financial support of the Dynasty Foundation. This work (N.S.A. and K.A.B.) was supported by the Government of Russia through the program P220 (project No 14.Z50.31.0021, leading scientist M. Bayer).

References

[1] I. B. Bersuker, The Jahn–Teller Effect (Cambridge University Press, Cambridge, 2006).

[2] V. V. Gudkov and I. B. Bersuker, in: Vibronic Interactions and the Jahn-Teller Effect, edited by M. Atanasov, C. Daul, and P. L. W. Tregenna-Piggott, Progress in Theoretical Chemistry and Physics B23 (Springer, Dordrecht, Heidelberg, London, New York, 2012), pp. 143–161.
[3] G. D. Watkins and J. W. Corbett, Phys. Rev. **134**, A1359 (1964).
[4] G. D. Watkins and J. R. Troxell, Phys. Rev. Lett. **44**, 593 (1980).
[5] D. Y. Jeon, H. P. Gislason, and G. D. Watkins, Phys. Rev. B **48**, 7872 (1993).
[6] F. C. Rong, W. A. Barry, J. F. Donegan, and G. D. Watkins, Phys. Rev. B **54**, 7779 (1996).
[7] V. Iota and B. A. Weinstein, Phys. Status Solidi B **211**, 91 (1999).
[8] Y. Q. Jui, N. J. Bardeleben, D. Stievenard, and C. Delerue, Phys. Rev. B **45**, 1645 (1992).
[9] N. S. Averkiev, A. A. Gutkin, and S. Yu Il'inskiy, Phys. Solid State **42**, 1231 (2000).
[10] N. K. Morosova, I. A. Karetnikov, V. V. Blinov, and E. M. Gavrischuk, Semiconductors **35**, 24 (2001).
[11] M. Ishikawa and T. Nakayama, Phys. Status Solidi C **10**, 1385 (2013).
[12] G. V. Colibaba and D. D. Nedeoglo, Moldavian J. Phys. Sci. **7**, 26 (2008).
[13] V. V. Gudkov and J. D. Gavenda, Magnetoacoustic Polarization Phenomena in Solids (Springer-Verlag, New York, Berlin, Heidelberg, 2000), pp. 27–31.
[14] V. Gudkov, A. Lonchakov, V. Sokolov, I. Zhevstovskikh, and N. Gruzdev, Phys. Status Solidi B **242**, R30 (2005).
[15] V. V. Gudkov, A. T. Lonchakov, V. I. Sokolov, I. V. Zhevstovskikh, and V. T. Surikov, Phys. Rev. B **77**, 155210 (2008).
[16] V. V. Gudkov, A. T. Lonchakov, V. I. Sokolov, I. V. Zhevstovskikh, and V. T. Surikov, Low Temp. Phys. **35**, 76 (2009).
[17] E. M. Georgy, M. D. Sturge, D. B. Fraser, and R. C. LeCraw, Phys. Rev. Lett. **15**, 19 (1965).
[18] M. D. Sturge, in: The Jahn–Teller Effect in Solids, edited by F. Seitz, D. Turnbull and H. Ehrenreich, Solid State Physics, Vol. 20 (Academic Press, New York and London, 1967), chap. II.
[19] T. Goto, H. Yamada-Kaneta, Ya. Saito, Yu. Nemoto, K. Sato, K. Kakimoto, and Sh. Nakamura, J. Phys. Soc. Jpn. **75**, 044602 (2006).
[20] K. Okabe, M. Akatsu, Sh. Baba, K. Mitsumoto, Yu. Nemoto, H. Yamada-Kaneta, T. Goto, H. Saito, K. Kashima, and Yo. Saito, J. Phys. Soc. Jpn. **82**, 124604 (2013).
[21] K. Mitsumoto, M. Akatsu, Sh. Baba, R. Takasu, Yu. Nemoto, T. Goto, H. Yamada-Kaneta, Yu. Furumura, H. Saito, K. Kashima, and Yo. Saito, J. Phys. Soc. Jpn. **83**, 034702 (2014).
[22] V. V. Gudkov, I. B. Bersuker, I. V. Zhevstovskikh, Yu. V. Korostelin, and A. I. Landman, J. Phys.: Condens. Matter **23**, 115401 (2011).